SUPPLEMENTAL MATERIAL

Zinselmeyer et al., http://www.jem.org/cgi/content/full/jem.20121416/DC1

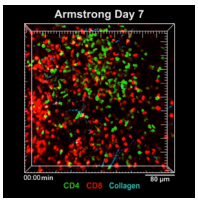

Video 1. Methodology to quantify antiviral T cell dynamics in the spleen. A representative time lapse of a 3D reconstruction shows the dynamics of CFP$^+$CD8$^+$ P14 cells (red) and GFP$^+$CD4$^+$ SMARTA cells (green) in the spleen 7 d after Arm infection. Collagen is show in cyan. The dotted line demarcates the border between the splenic white (WP) and red pulp (RP). Antiviral T cell dynamics were quantified separately in these two distinct anatomical regions.

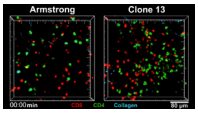

Video 2. Analysis of early splenic antiviral T cell dynamics after acute versus persistent viral infection. Two representative time lapses of 3D reconstructions show CD8$^+$ P14 cells (red), CD4$^+$ SMARTA cells (green), and collagen (cyan) in the spleen 4 d after infection with Arm or CL13. The dotted lines demarcate the border between the splenic white and red pulp.

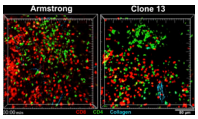

Video 3. Splenic antiviral T cell dynamics during acute versus persistent viral infection. (Part 1) Two representative time lapses of 3D reconstructions show CD8$^+$ P14 cells (red), CD4$^+$ SMARTA cells (green), and collagen (cyan) in the spleen 7 d after infection with Arm or CL13. The dotted lines demarcate the border between the splenic white and red pulp. White boxes denote areas of higher magnification shown in part 2. (Part 2) Time lapses showing higher magnifications of the areas denoted in part 1.

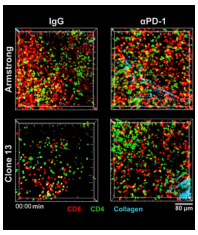

Video 4. Anti–PD-1 enhances the motility of antiviral T cells during persistent viral infection. Representative time lapses of 3D reconstructions show CD8$^+$ P14 cells (red), CD4$^+$ SMARTA cells (green), and collagen (cyan) in the spleen 7 d after infection with Arm or CL13. Sixteen hrs before imaging, mice were injected intravenously with either anti–PD-1 or isotype control antibodies. The dotted lines demarcate the border between the splenic white and red pulp.

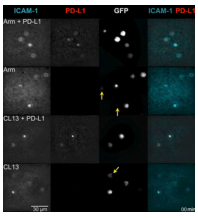

Video 5. PD-L1 promotes CD8+ T cell synapse formation. After a 10-min incubation on the bilayer, TIRFM was used to visualize GFP$^+$ P14 cell interactions with planar bilayers loaded with H-2D^{b}GP$_{33-41}$ (unlabeled) and ICAM-1^{AF405} (cyan) in the presence or absence of PD-L1^{AF568} (red). Representative time lapses (36 min duration; 4-min intervals) show the entire xy field of view. Yellow arrows denote GFP$^+$ P14 cells that are moving/crawling during the time lapse. Note the increased number of moving/crawling (or, kinapses) GFP$^+$ P14 cells in the absence of PD-L1, both for Arm and CL13. In contrast, the presence of PD-L1 on the bilayer promotes stable synapse formation. Time-lapses are representative of three independent experiments.

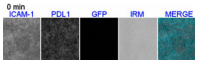

Video 6. PD-L1 centralizes to the cSMAC during synapse formation. A representative time-lapse captured by TIRFM shows the movement of PD-L1^{AF568} (red) to the cSMAC and ICAM-1^{AF405} (cyan) to the pSMAC after engagement of a day 7 Arm GFP$^+$ P14 cell with a planar bilayer. The video shows a 40-min time-course (4-min intervals) initiated immediately after P14 cells were loaded onto the bilayer. IRM (interference reflection microscopy) denotes the reflection image of the P14 cell on the bilayer. The time lapse is representative of two independent experiments.